Available online at www.sciencedirect.com
SCIENCE DIRECT®
Journal of Magnetic Resonance 163 (2003) 369–373
JMR Journal of Magnetic Resonance
www.elsevier.com/locate/jmr

Communication

Rotating-frame spin–lattice relaxation time imaging by radio-frequency field gradients: visualization of strained crosslinked natural rubbers

H. Chaumette, D. Grandclaude, and D. Canet*

Laboratoire de Méthodologie RMN,[1] *Faculté des Sciences, Université Henri Poincaré, Nancy 1, B.P. 239, Vandoeuvre-lès-Nancy 54506, France*

Received 17 February 2003; revised 14 April 2003

Abstract

NMR imaging by radio-frequency field gradients (B_1 gradients) is especially convenient for heterogeneous samples and/or in the case of relatively short transverse relaxation times. The method has been combined with the application of two spin-lock periods of different duration so as to produce rotating-frame spin–lattice relaxation time ($T_{1\rho}$) images. In the case of natural rubber samples with different crosslink densities, such images are not only characteristic of the crosslink density but also reveal the way in which the material has been stressed. The strained parts can be visualized either directly or through histograms showing the $T_{1\rho}$ distribution over the whole sample.

In spite of the claimed potentiality of NMR images displaying values of the rotating-frame spin–lattice relaxation time ($T_{1\rho}$) rather than of spin density [1,2], the method has not yet gained a wide recognition, as compared with transverse relaxation time images [3]. This may appear surprising as $T_{1\rho}$ is devoid of problems associated with the measurement of the transverse relaxation time, T_2, yet leading in principle to the same type of information. These problems include echo modulation by spin–spin couplings, possibly composite decays (Gaussian and multiexponential) and experimental difficulties related to the quality of radio-frequency (RF) pulses [4]. In fact, if one is primarily interested in contrasts arising from slow motions, $T_{1\rho}$ would be even more informative than T_2 since its inverse is dominated by a spectral density not at zero frequency (T_2 case), but at a frequency given by

$$\nu_1 = \frac{\gamma B_1}{2\pi}, \tag{1}$$

where γ is the gyromagnetic ratio of the considered nucleus and B_1 is the amplitude of the spin-locking RF field used for letting the system evolve under $T_{1\rho}$. The usual values of B_1 are such that ν_1 lies in the 1–100 kHz range, thus rendering $T_{1\rho}$ sensitive to motions having a characteristic time in the millisecond–microsecond range. Identification of those motions can be achieved through dispersion imaging, that is pixel-by-pixel evolution of $T_{1\rho}$ as a function of ν_1. This feature has been exploited for different proton systems which include slowly moving macromolecules or paramagnetic contrast agents [2], crosslinked rubbers [5,6], and articular cartilage [7]. Concerning crosslinked rubbers, the subject of the present paper, the question is to decide whether it is necessary to probe the whole dispersion curve in order to achieve a significant characterization of the material. In previous papers [8,9], it has been shown experimentally that these dispersion curves exhibit systematically a decrease of $T_{1\rho}$ with ν_1 while they appear approximately parallel, their respective shift increasing with the crosslink density. This means that a proper discrimination can be obtained at any reasonable value of ν_1 (say 10 kHz). From an interpretation point of view, dispersion curves could be fitted according to

$$R_{1\rho} = k_0 + \frac{k_1}{\nu_1^{\alpha}}, \tag{2}$$

* Corresponding author. Fax: +33-3839-12367.
E-mail address: daniel.canet@rmn.uhp-nancy.fr (D. Canet).
[1] FRE CNRS 2415, INCM-FR CNRS 1742.

1090-7807/$ - see front matter © 2003 Elsevier Science (USA). All rights reserved.
doi:10.1016/S1090-7807(03)00143-5

where the relaxation rate $R_{1\rho}$ is the inverse of $T_{1\rho}$ and where k_0 and k_1 are both proportional to the mean square of *residual proton–proton dipolar couplings* (in other words to the second moment of the proton resonance line). α, the exponent of the power law, has to be experimentally determined [5,8] and was found to be the same for all samples in the series previously investigated [8]. Moreover, T_1 dispersion curves published quite recently on similar systems [10] are comparable to $T_{1\rho}$ dispersion curves; this comparison is of course valid in the limited frequency range allowed by $T_{1\rho}$ measurements where only the effects of slow motions can be probed. The important point is that $T_{1\rho}$, measured with a given B_1 amplitude is characteristic of the values of residual dipolar couplings which are themselves related to crosslink density.

It looks therefore interesting to devise an imaging experiment based on $T_{1\rho}$ values or $T_{1\rho}$ distribution so as to visualize possible heterogeneities within a rubber sample. Such experiments employing B_0 gradients already exist [1,2,5–8]; they imply of course a period of spin-lock ending by a $\pi/2$ pulse which flips back the magnetization toward the z axis where it is stored before being imaged. This is followed by a spoil gradient in order to suppress any transverse magnetization; thereafter the imaging process can start.

However, performing $T_{1\rho}$ imaging with B_1 gradients turns out to be much simpler. The method follows from previous procedures aimed at obtaining T_1 or T_2 images [11,12] and relies on two interleaved experiments with two different relaxation evolution intervals. The basic sequence is shown in Fig. 1 where the standard acquisition stage is simply replaced by a train of short B_1 gradient pulses with acquisition of a single point between two consecutive pulses. The Fourier transform of the pseudo-fid which has been obtained that way yields the spatial profile of the projection upon the B_1 gradient direction [13]. A 2D map is obtained by a step-by-step sample rotation and a treatment based on the projection–reconstruction principle along with an adaptation of the "filtered back projection" algorithm [14]. A $T_{1\rho}$ map is obtained by a pixel-by-pixel analysis of the two data sets corresponding, respectively, to the two evolution intervals of duration τ_1 and τ_2, recognizing that the interleaved mode affords compensation for any instrumental drift. If we denote by I_1 and I_2 the intensities associated with τ_1 and τ_2, respectively, we have

$$T_{1\rho} = \frac{\tau_1 - \tau_2}{\ln(I_2/I_1)}. \tag{3}$$

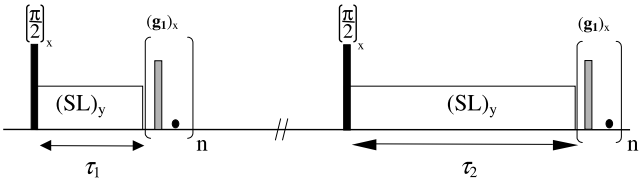

Fig. 1. Sequence used for the generation of $T_{1\rho}$ maps. $(SL)_y$ indicates a spin-lock period; $(g_1)_x$ symbolizes a B_1 gradient pulse repeated n times so that a pseudo-fid representative of spatial encoding is acquired one data point at a time (indicated by the dot between two consecutive gradient pulses).

The four rubber samples studied here (denoted in the following by G, A, B, and C) are small cylinders of approximately 3 mm diameter cut from plates of 2 mm thickness kindly provided by Hutchinson S.A. (Châlette-sur-Loing, France). They differ by their amounts of sulfur and CBS (*N*-cyclohexylbenzothiazole-2-sulfenamide, which is a vulcanization accelerator). G is natural rubber without any treatment whereas A, B, and C have been vulcanized with 1, 2, and 3 phr (per hundred rubber), respectively, of both sulfur and CBS. Crosslink density thus increases from G to A, B, and C. ^{1}H NMR experiments have been carried out with a homemade spectrometer operating at 200 MHz, equipped with a special probe capable of delivering a radio-frequency field gradient of approximately 20 G/cm. The sample placed in a NMR tube was rotated by steps of 3.6°; this yields a hundred profiles from which $T_{1\rho}$ images were reconstructed (pixels for which the spin density is lower than 20% of the maximum intensity were disregarded since, in these conditions, $T_{1\rho}$ determination is unreliable). The amplitude of the spin-lock field was adjusted so that $\nu_1 = 10$ kHz; τ_1 and τ_2 were set at 1 and 4 ms, respectively.

At first glance, images displayed in Fig. 2 are representative of the mean $T_{1\rho}$ value pertaining to each sample. This mean value is indeed close to the result obtained from conventional $T_{1\rho}$ measurements (obtained with larger pieces of rubber, more gently cut than the samples investigated here) but systematically lower (see Table 1). This feature can be easily understood by considering the histograms [5,6] which are seen to be systematically asymmetrical with the extended part toward smaller $T_{1\rho}$ values. This asymmetry decreases from G to C, just as the deviation between conventional $T_{1\rho}$ values and those extracted from images. In spite of these deviations, a simple look at the colors of images in Fig. 2 indicates that crosslink density discrimination can be simply and reliably achieved through two spin-lock experiments with properly chosen evolution times (τ_1 and τ_2).

Also interesting is the $T_{1\rho}$ distribution within each sample which is seen to involve a marked decrease on the edges of the pieces of rubber, at least for the softer materials (samples G and A). Smaller $T_{1\rho}$ values indicate larger residual dipolar interactions [9] which obviously do not arise from a change of crosslink density but rather from a reduced distance between interacting protons or from an increase in chain rigidity; one can naturally envision that this can be produced by polymeric chains becoming closer and this is indeed what

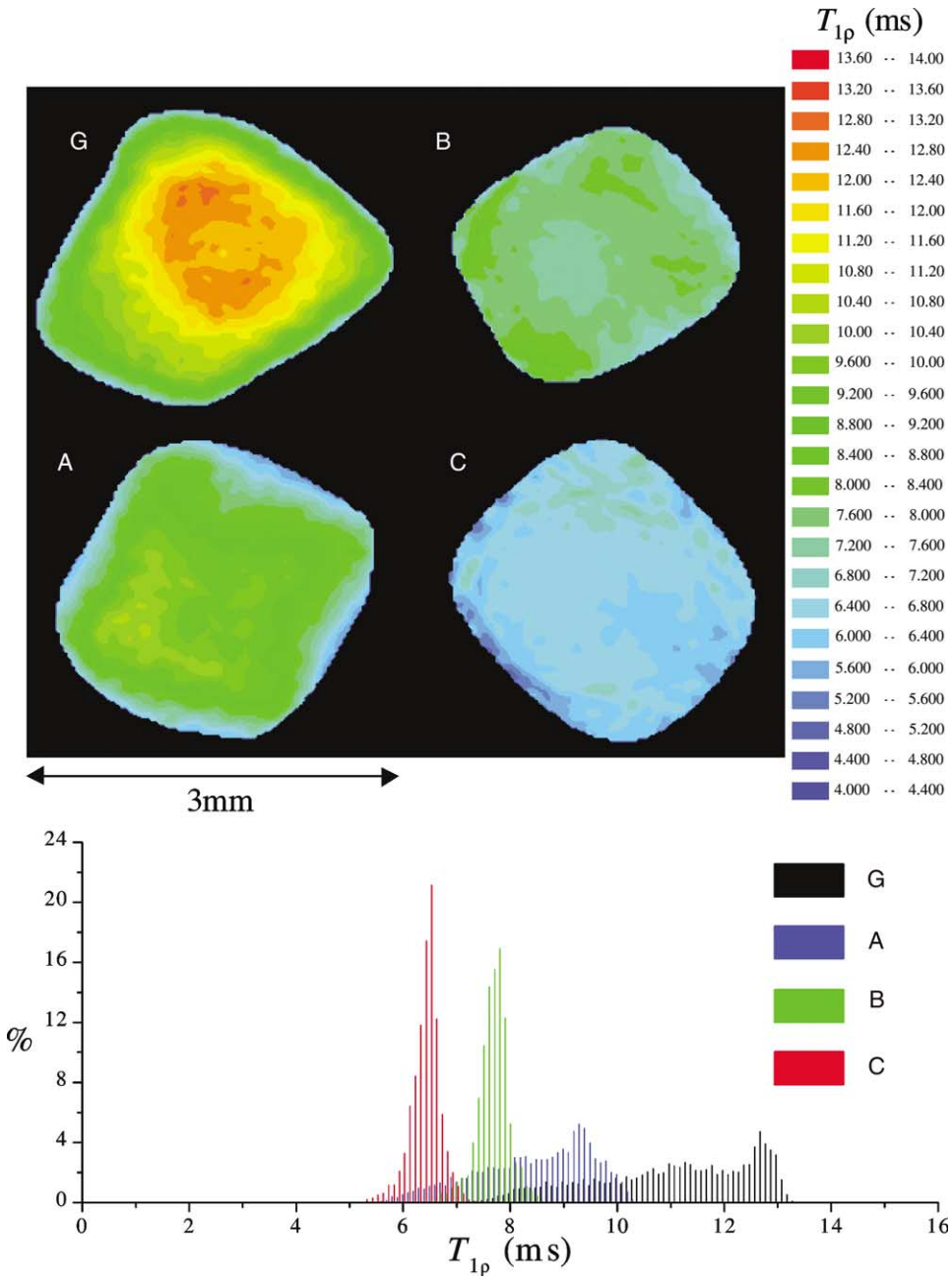

Fig. 2. $T_{1\rho}$ maps for the four rubber samples which differ by their crosslink density (see text), along with the corresponding histograms showing the $T_{1\rho}$ dispersal for each sample. The color scale is common permitting a direct comparison of the four images.

Table 1
Comparison of mean $T_{1\rho}$ values (ms) extracted from the images of Fig. 2 with values determined from a conventional measurement

Sample	Conventional	Image
G	13.4 ± 0.7	11.5 ± 0.8
A	9.4 ± 0.5	8.5 ± 0.6
B	8.3 ± 0.4	7.7 ± 0.6
C	6.9 ± 0.4	6.2 ± 0.6

occurs in the regions of lowest $T_{1\rho}$ values which are also the regions of stress since samples have been punched from the rubber plate.

Sample heterogeneity is still better appreciated from the images and histograms of Fig. 3 which are a representation of reduced and centered data, $(T_{1\rho} - \overline{T_{1\rho}})/\overline{T_{1\rho}}$, $\overline{T_{1\rho}}$ being the mean value for the considered sample. The strained regions (sample edges) are clearly visible for sample G (natural rubber without any treatment) and sample A (lowest crosslink density), while they are virtually absent in images of samples B and C. It can be seen that histograms corresponding to these two undamaged samples are symmetrical (with this representation) and presumably reflect the random distribution of crosslinks and/or measurement uncertainties.

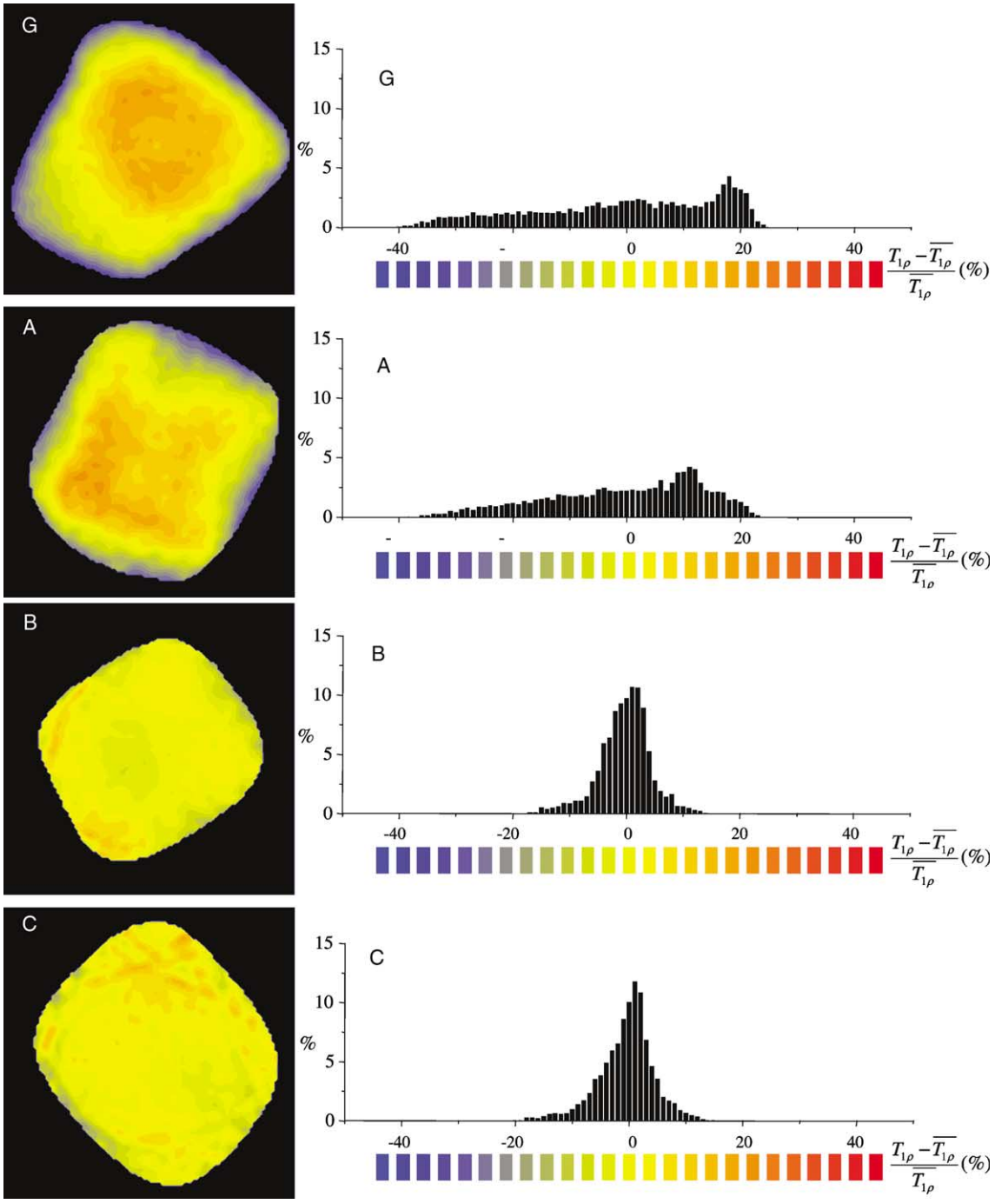

Fig. 3. Same as Fig. 2 with reduced and centered data $((T_{1\rho} - \overline{T_{1\rho}})/\overline{T_{1\rho}})$ which afford a better visualization of sample heterogeneity.

Conversely, histograms for samples G and A remain asymmetrical and much broader indicating unambiguously a non-random lowering of $T_{1\rho}$ in strained regions. These regions are wider in the case of samples A and G because they are soft rubbers (G, untreated; A, lowest crosslink density) and consequently are prone to be more altered than the other samples in the series.

NMR methods have been used for long in order to characterize stressed materials [3]. The approach developed here has the merit of simplicity and efficiency, probably due to the fact that it employs B_1 gradients, known to be well adapted to systems with relatively short transverse relaxation times. Moreover, imaging methods based on this type of gradients do not suffer from abrupt modifications of magnetic susceptibility [15] as the ones existing at the sample edges; it is therefore especially well suited for observing subtle changes occurring in regions close to an interface.

References

[1] E. Rommel, R. Kimmich, Volume-selective determination of the spin-lattice relaxation time in the rotating frame, $T_{1\rho}$, and $T_{1\rho}$ imaging, Magn. Reson. Med. 12 (1989) 209–218.

[2] E. Rommel, R. Kimmich, $T_{1\rho}$ dispersion imaging and volume-selective $T_{1\rho}$ dispersion weighted NMR spectroscopy, Magn. Reson. Med. 12 (1989) 390–399.

[3] B. Blümich, NMR Imaging of Materials, Clarendon Press, Oxford, 2000.

[4] R. Kimmich, NMR Tomography, Diffusometry, Relaxometry, Springer, Berlin, 1997.

[5] P. Barth, S. Hafner, P. Denner, Material property NMR imaging of cross-linked polymers based on longitudinal relaxation in the rotating frame, Macromolecules 29 (1996) 1655–1659.

[6] P. Barth, S. Hafner, Investigation of aging in polymer networks by $T_{1\rho}$ material property NMR imaging, Magn. Reson. Imaging 15 (1997) 107–112.

[7] S.V.S. Akella, R.R. Regatte, A.J. Gougoutas, A. Borthakur, E.M. Shapiro, J.B. Kneeland, J.S. Leigh, R. Reddy, Proteoglycan-induced changes in $T_{1\rho}$-relaxation of articular cartilage at 4T, Magn. Reson. Med. 46 (2001) 419–423.

[8] H. Chaumette, D. Grandclaude, P. Tekely, D. Canet, C. Cardinet, A. Verschave, Characterization of cross-linked rubber materials via proton rotating-frame relaxation measurements, J. Phys. Chem. A 105 (2001) 8850–8856.

[9] H. Chaumette, D. Grandclaude, J. Brondeau, L. Werbelow, D. Canet, Rotating-frame spin lattice relaxation measurements ($T_{1\rho}$) with weak spin-locking fields in the presence of homonuclear dipolar coupling, Mol. Phys., in press.

[10] S. Kariyo, S. Stapf, Influence of cross-link density and deformation on the NMR relaxation dispersion of natural rubber, Macromolecules 35 (2002) 9253–9255.

[11] F. Humbert, E. Collenne, M. Valtier, D. Canet, Nuclear longitudinal relaxation time images by radiofrequency field gradients, J. Magn. Reson. 138 (1999) 164–166.

[12] C. Malveau, D. Grandclaude, D. Canet, Nuclear relaxation time images by radiofrequency field gradients applied to the study of solvent permeation into polymeric materials, J. Magn. Reson. 150 (2001) 214–218.

[13] D. Canet, Radiofrequency field gradient experiments, Prog. Nucl. Magon. Reson. Spectrosc. 30 (1997) 101–135.

[14] P. Maffei, P. Mutzenhardt, A. Retournard, B. Diter, R. Raulet, J. Brondeau, D. Canet, NMR microscopy by radiofrequency field gradients, J. Magn. Reson. A 107 (1997) 40–49.

[15] R. Raulet, J.M. Escanyé, F. Humbert, D. Canet, Quasi-immunity of B_1 gradient NMR microscopy to magnetic susceptibility distortions, J. Magn. Reson. A 119 (1996) 111–114.